This paper is published as part of a *Dalton Transactions* themed issue on:

The Synergy between Theory and Experiment

Guest Editor John McGrady
University of Glasgow, UK

Published in issue 30, 2009 of *Dalton Transactions*

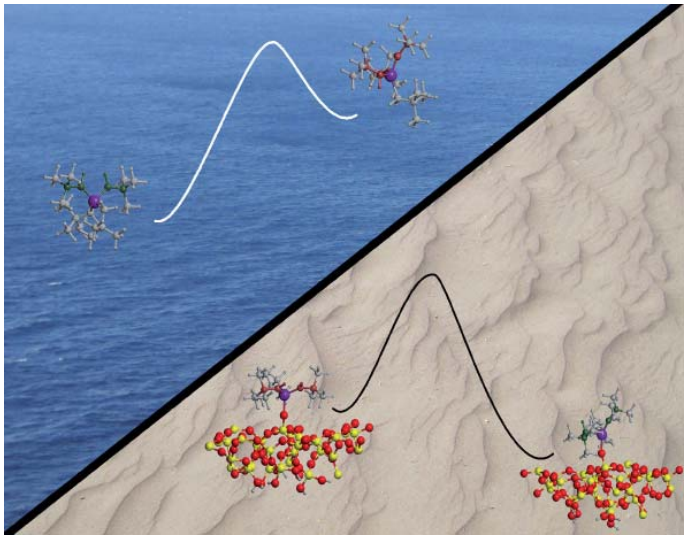

Image reproduced with permission of Christophe Coperet

Papers published in this issue include:

A combined picture from theory and experiments on water oxidation, oxygen reduction and proton pumping
Per E. M. Siegbahn and Margareta R. A. Blomberg, *Dalton Trans.*, 2009,
DOI: 10.1039/b903007g

Mechanisms of C–H bond activation: rich synergy between computation and experiment
Youcef Boutadla, David L. Davies, Stuart A. Macgregor and Amalia I. Poblador-Bahamonde, *Dalton Trans.*, 2009,
DOI: 10.1039/b904967c

Are tetrathiooxalate and diborinate bridged compounds related to oxalate bridged quadruply bonded compounds of molybdenum?
Malcolm H. Chisholm and Namrata Singh, *Dalton Trans.*, 2009
DOI: 10.1039/b901734h

Molecular recognition in Mn-catalyzed C–H oxidation. Reaction mechanism and origin of selectivity from a DFT perspective
David Balcells, Pamela Moles, James D. Blakemore, Christophe Raynaud, Gary W. Brudvig, Robert H. Crabtree and Odile Eisenstein, *Dalton Trans.*, 2009
DOI: 10.1039/b905317d

Visit the *Dalton Transactions* website for more cutting-edge inorganic and organometallic research
www.rsc.org/dalton

Crystal structure of octabromoditechnetate(III) and a multi-configurational quantum chemical study of the δ → δ* transition in quadruply bonded $[M_2X_8]^{2-}$ dimers (M = Tc, Re; X = Cl, Br)†

Frederic Poineau,*[a] Laura Gagliardi,[b,c] Paul M. Forster,[a] Alfred P. Sattelberger[a,d] and Kenneth R. Czerwinski[a]

Received 2nd February 2009, Accepted 3rd April 2009
First published as an Advance Article on the web 8th May 2009
DOI: 10.1039/b902106j

The technetium(III) compound $(n\text{-}Bu_4N)_2[Tc_2Br_8]$ was prepared by metathesis of $(n\text{-}Bu_4N)_2[Tc_2Cl_8]$ with concentrated aqueous HBr in acetone and recrystallized from acetone–diethyl ether solution (2 : 1 v/v). The acetone solvate obtained, $(n\text{-}Bu_4N)_2[Tc_2Br_8]\cdot 4[(CH_3)_2CO]$ (**1**), crystallizes in the monoclinic space group $P2_1/n$ with $a = 13.8959(8)$ Å, $b = 15.2597(9)$ Å, $c = 15.5741(9)$ Å, $\beta = 109.107(1)°$, $R_1 = 0.028$, and $Z = 4$. The Tc–Tc distance (2.1625(9) Å) and the average Tc–Br distances (2.4734(7) Å) are in excellent agreement with those previously determined by EXAFS spectroscopy. These and other experimental data on quadruply metal–metal bonded group 7 $[M_2X_8]^{2-}$ dimers (M = Tc, Re; X = Cl, Br) are compared to the results of a set of multi-configurational quantum chemical studies. The calculated molecular structures of the ground states are in very good agreement with the structures determined experimentally. The theory overestimates the δ → δ* transition energies by some 1 000 cm^{-1}, but mimics the trends in δ → δ* energies across the series.

Introduction

An understanding of molecular compounds that contain metal–metal bonds is fundamental to interpreting structural and bonding properties, catalysis, metal surface chemistry, and magnetism.[1] The discovery of dirhenium(III) complexes with metal–metal quadruple bonds foreshadowed a revolution in the study of metal–metal bonds and the identification of novel types of bonding.[2] The importance of quantum chemistry to this area of science is not only based on its ability to solve the quantum-mechanical equations to a good degree of approximation for complex molecules, but also on the fact that the field can now perform theoretical simulations of real benefit to the experimental community. *Ab initio* quantum chemistry has made so many advances in the last 40 years that it now allows the study of molecular systems containing any of the atoms in the periodic table. Technetium chemistry represents a challenge for experimentalists and the interplay between theory and experiment is of extreme importance in such a case. In the following, we present a combined experimental and theoretical study in which we elucidate some key features of the Tc–Tc quadruple bond.

[a]*Department of Chemistry, University of Nevada Las Vegas, Las Vegas, NV 89154, USA. E-mail: freder29@unlv.nevada.edu*
[b]*Department of Physical Chemistry, Sciences II University of Geneva, 30 Quai Ernest Ansermet, CH-121, Geneva, Switzerland. E-mail: laura.gagliardi@chiphy.unige.ch*
[c]*University of Minnesota Department of Chemistry and Supercomputing Institute, 207 Pleasant St., SE Minneapolis, MN MN 55455-0431, USA*
[d]*Energy Sciences and Engineering Directorate, Argonne National Laboratory, Argonne, IL 60439, USA*

† Electronic supplementary information (ESI) available: Additional crystallographic tables and X-ray crystallographic data for **1**, as well as the CASPT2 total energies for $[M_2X_8]^{2-}$ (M = Tc, Re; X = Cl, Br) and the coordinates of the optimized structures. CCDC reference number 720059. For ESI and crystallographic data in CIF or other electronic format see DOI: 10.1039/b902106j

Exploration of the fundamental chemistry of technetium remains limited due to the relatively small number of laboratories equipped to work with suitable quantities of this fascinating radioelement. Over the past three years, we have established the capability to work with synthetic quantities (*i.e.*, multi-milligram amounts) of ^{99}Tc in the radiological laboratories of the Harry Reid Center for Environmental Studies at UNLV and have been exploring several aspects of its inorganic and organometallic chemistry. One of our interests is multiply metal–metal bonded technetium complexes for which there is a paucity of data in the primary literature. As one striking comparison with its heavier congener, more than one hundred quadruply metal–metal bonded rhenium(III) dimers have been crystallographically characterized, while only five such examples are known for technetium.[3,4] In fact, it has been more than 15 years since the last crystal structure of a Tc(III) dimer, that of $Tc_2(O_2CCH_3)_4(TcO_4)_2$, was reported.[5] Recently, we presented structural data for the $[Tc_2X_8]^{2-}$ ions (X = Cl, Br) derived from analysis of EXAFS spectra of the tetra-*n*-butyl ammonium (TBA) salts, as well as the electronic spectra of the two octahaloditechnetate ions in solution.[6] The close similarity of the optical spectra with those of their rhenium analogues permitted an assignment of the electronic transitions in the $[Tc_2X_8]^{2-}$ dimers, including the ubiquitous δ → δ* transitions. Of particular note was the near coincidence of the δ → δ* transitions in the $[M_2Cl_8]^{2-}$ and $[M_2Br_8]^{2-}$ complexes (M = Tc, Re). It occurred to us that calculations of the electronic spectra of these dimers had never been pursued simultaneously using state-of-the-art methods. This situation is partially remedied in the present work. We have performed multi-configurational quantum chemical calculations, using the Complete Active Space SCF (CASSCF) method, followed by second order perturbation theory (CASPT2) to determine: (1) the structures of the $[M_2X_8]^{2-}$ complexes in their $^1A_{1g}$ ground states and $^1A_{2u}$ excited states, (2) the energies and trends associated with the δ → δ* transitions,

and (3) the bond order of the metal–metal bonds in each complex. Finally, the structure of the $[Tc_2Br_8]^{2-}$ ion as an acetone solvate, $(n\text{-}Bu_4N)_2[Tc_2Br_8]\cdot 4[(CH_3)_2CO]$ (**1**), was determined by single-crystal X-ray diffraction and compared to the geometry derived from the aforementioned EXAFS data.

Experimental

Synthesis

Caution. Techetium-99 is a weak beta emitter (E_{max} = 292 keV). All manipulations were performed in a radiochemistry laboratory designed for chemical synthesis using efficient HEPA-filtered fume hoods, Schlenk and glove box techniques, and following locally approved radioisotope handling and monitoring procedures. The compound $(n\text{-}Bu_4N)_2[Tc_2Br_8]$ was prepared according to the procedure previously reported.[7] Single crystals suitable for X-ray diffraction were grown over the course of 1 week from a concentrated acetone solution of the salt that was carefully layered with diethyl ether (2 : 1 v/v) at –25 °C.

Crystal structure determination

Initial attempts to determine the structure of $(n\text{-}Bu_4N)_2[Tc_2Br_8]$ utilized samples that had been removed from the mother liquor for a few hours. While the samples appeared crystalline to the naked eye, only weak diffraction peaks were observed. Suspecting desolvation, a clear crystal was selected directly from the mother liquor and quickly moved by needle into a drop of paratone oil. The paratone-covered crystal was then mounted on a glass fiber and immediately cooled in a nitrogen cold stream to 150 K. A full hemisphere of data was then collected on a Bruker APEX II diffractometer. The structure was solved by direct methods and refined against F^2 using SHELX-97.[8] Hydrogen atoms were added geometrically and refined using the riding model. The data to parameter ratio is only slightly higher than the ideal 10 : 1 ratio. This is undoubtedly a result of a more significant decrease in scattering intensity at high scattering vectors than usual, due to poorly ordered solvent molecules in the lattice (see below), and necessitating a data cutoff after integration at 0.88 Å^{-1} in the final refinement. Fourier peaks suggested positional disorder in **1**. Within **1**, it is possible for the Tc–Tc bond to point in three separate directions (details are presented in the Results and Discussion section). In the final refinement, it was found that a dominant Tc–Tc pair is present with 91.96 refined occupancy, while the less favorable orientations refine to 5.01 and 3.03%, respectively. Given the approximately cubic dimensions of the dimer, no partially ordered models were needed for the Br positions. The value for the three occupancies was constrained to be equal to 1 total. No other constraints/restraints were needed to obtain a reasonable structure for non-hydrogen atoms. The structure refined down to an R_1 value of 2.80%. Refinement to a chemically reasonable geometry, displacement parameters, and bond distances for the TBA cation suggests a very reliable structure determination overall, especially considering how poorly TBA often orders. The displacement parameters for all molecules are generally good with the exception of one of the two crystallographically independent acetone molecules. The large displacement parameters for this molecule are suggestive of a poorly defined crystallographic position for the molecule itself, as is chemically sensible based on the crystal structure, rather than a low quality crystal structure determination. An attempt at refining the acetone with the largest displacement parameters using partial occupancy lead to a refined occupancy parameter slightly above unity, indicative of disorder rather than partial occupancy. Selected crystallographic information is presented in Table 1, full crystallographic information and a cif file are supplied in the ESI.†

Table 1 Crystallographic parameters for $(n\text{-}Bu_4N)_2[Tc_2Br_8]\cdot 4[(CH_3)_2CO]$

Formula	$C_{44}H_{96}Br_8N_2O_4Tc_2$
M_r/g mol^{-1}	1554.49
Crystal system	Monoclinic
Space group	$P2_1/n$
a/Å	13.8959(8)
b/Å	15.2597(9)
c/Å	15.5741(9)
α/°	90
β/°	109.107(1)
γ/°	90
V/Å^3	3120.5(3)
Z	4
ρ/g cm^{-3}	1.652
T/K	150(2)
Radiation	Mo Kα
Wavelength	0.71073
Reflections collected	5630
Independent reflections	2907
Parameters	280
Largest diffraction peak/e Å^{-3}	0.612
$R(F_o)(F_o^2 > 2\sigma(F_o^2))$	0.0280
$R(F_o^2)$ (all data)	0.0365
$R_w(F_o^2)$	0.0696
Goodness-of-fit	1.008

Computational details

All calculations were performed using the MOLCAS-7.2 package.[9] The ANO-RCC basis set was used for all atoms.[10] Two sets of calculations were performed, one with basis sets of VTZP quality and one with VQZP quality. The VTZP basis corresponds to the following contractions: 8s7p5d3f2g1h for Re, 7s6p4d2f1g for Tc, 5s4p2d1f for Cl and 6s5p3d1f for Br. The VQZP basis corresponds to the contractions: 9s8p6d4f3g2h for Re, 8s7p5d3f2g1h for Tc, 6s5p3d2f1g for Cl and 7s6p4d2f1g for Br. The complete active space CASSCF method is used to generate wave functions for a predetermined set of electronic states.[11] Dynamic correlation is added using second-order perturbation theory, CASPT2.[12] Scalar relativistic effects were included using a Douglas–Kroll–Hess Hamiltonian.[13] The geometry of the $^1A_{1g}$ ground state of the complexes was initially taken from crystallographic data.[6,14–16] A numerical optimization of two degrees of freedom, the metal–metal (M–M) and metal–halide (M–X) bond distances was then performed for both the $^1A_{1g}$ ground state and the $^1A_{2u}$ excited state at the CASPT2 level, using the VTZP basis and assuming that the complexes had rigorous D_{4h} symmetry. Because MOLCAS works in subgroups of the D_{2h} point group, all calculations were performed in D_{2h} symmetry. The adiabatic energy difference between the $^1A_{1g}$ and $^1A_{2u}$ electronic states was computed with both the VTZP basis set and VQZP basis set at the VTZP optimized geometries. In the CASSCF calculations the complete active space contains twelve electrons in twelve active orbitals (12/12). This

space comprises one ndσ, two ndπ, and one ndδ M–M bonding orbitals and the corresponding antibonding orbitals, two M–X δ bonding orbitals and the corresponding two antibonding MOs. This active space can only describe electronic states where the excitations are located in the M–M bond. All the Cl 3p (Br 4p) orbitals should be included in the active space to cover also all possible ligand-to-metal charge-transfer (LMCT) excitations, but these excitations have not been considered in the present study. In the subsequent CASPT2 calculations, orbitals up to and including the 4d for Re, 3d for Tc, 2p for Cl and 3p for Br were kept frozen. The method has proven to be successful in the study of similar systems.[17–21] The molecular orbitals forming the active space for $Tc_2Br_8^{2-}$ are shown in Fig. 1.

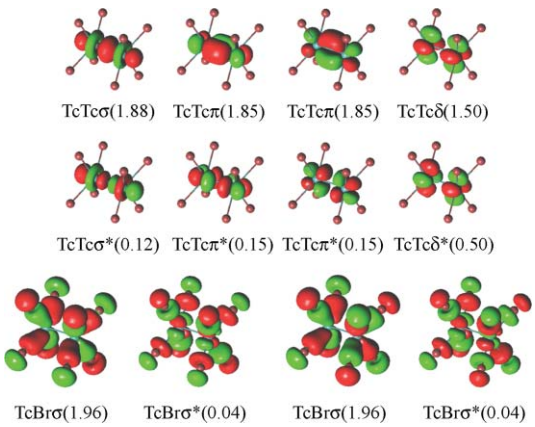

Fig. 1 Active orbitals for $[Tc_2Br_8]^{2-}$ with their occupation numbers in the ground state.

Results and discussion

The TBA salt of octabromoditechnetate(III) crystallizes as an acetone solvate in the monoclinic space group $P2_1/n$. The asymmetric unit contains two acetone molecules, one tetrabutylammonium cation and one half of a $Tc_2Br_8^{2-}$ anion that is completed by an inversion operation. The absence of highly favorable intermolecular interactions between the three constituents of the material leads to a structure best described as folded sheets of TBA cations with 1D cavities occupied by $[Tc_2Br_8]^{2-}$ anions and acetone (Fig. 2a). The $[Tc_2Br_8]^{2-}$ anions only fill the 1D voids partially, resulting in the inclusion of two acetone solvent molecules between anions (Fig. 2b). The large displacement parameters of the acetone, coupled with the observation that there are no strong intra molecular interactions between acetone and other species, suggests its role is primarily to occupy space. The TBA cations assume a relatively flat geometry in the puckered sheets to maximize Van der Waals interactions between the interdigitated butyl chains (Fig. 3). Voids in this arrangement are occupied by a second crystallographically unique acetone molecule. The moderately lower displacement parameters on this acetone molecule indicate it is more significant for stabilizing the structure overall. Views using space-filling representations (not shown) indicate that the molecules are in Van der Waals contact within the sheets.

Disordering of $M_2X_8^{2-}$ anions in $(n\text{-}Bu_4N)_2M_2X_8$ crystal structure has already been observed for the rhenium (X = Cl, Br) and technetium analogues (X = Cl).[14–16] For the chloride

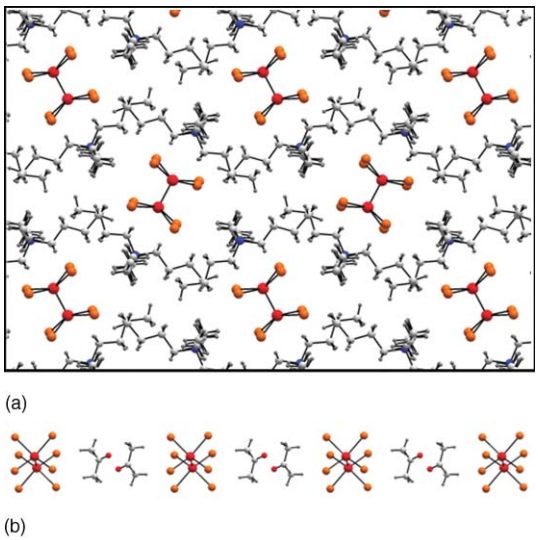

Fig. 2 (a) Structural view of **1** from the *a* crystallographic direction. Tc, Br, N, C and H atoms are in orange, red, blue, grey, and dark grey, respectively. Acetone solvent molecules and low occupancy Tc1b and Tc1c sites are not shown for clarity. (b) View of the anion arrangement in **1** from the *b* crystallographic direction. Tc, Br, C, and H atoms are in orange, red, grey, and dark grey, respectively.

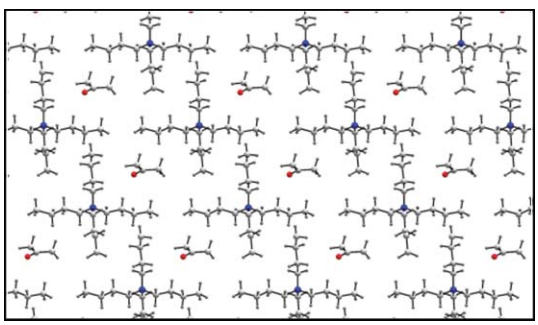

Fig. 3 Structural view of the TBA sheets from **1**, viewed in the *b* crystallographic direction. N, C and H atoms are in blue, grey, and white, respectively.

analogue $(n\text{-}Bu_4N)_2[Tc_2Cl_8]$, the anions are disordered such that ~30% of the $[Tc_2Cl_8]$ units are perpendicular to the majority orientation.[14] While not intuitive, the 8 Br atoms in $[Tc_2Br_8]^{2-}$ form an approximate cube, with the longest Br–Br distance varying approx. 2% between shorter Br–Br distances for Br atoms on the same Tc atom *vs.* Br–Br distances for Br atoms across the Tc–Tc quadruple bond from one another. Presumably, the energy difference between differing orientations of the nearly cubic anion in these structures is sufficiently low that multiple orientations are typically observed. In the case of **1**, the disorder is sufficiently low (~8%) that there should be minimal distortion of the Tc–Tc bond distance, consistent with its agreement with the EXAFS data. For the alternate orientations, the Tc–Tc bond distances are roughly 0.1 Å lower, indicating that their occupancy is too low for physically meaningful bond distances to be extracted. The presence of acetone increases the unit cell volume and **1** has the highest unit cell volume among the four $(n\text{-}Bu_4N)_2[M_2X_8]$ (M = Tc, Re; X = Cl, Br) compounds.[14–16] The $[Tc_2Br_8]^{2-}$ anion (Fig. 4) exhibits an eclipsed geometry comparable

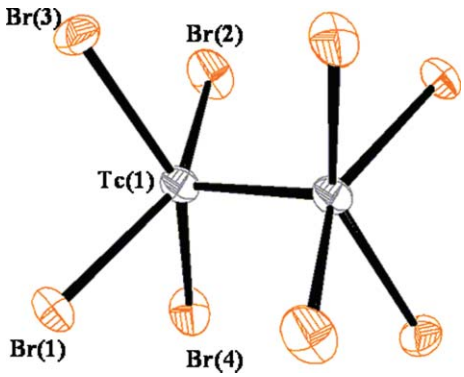

Fig. 4 ORTEP representation of the $Tc_2Br_8^{2-}$ ion in $(n\text{-}Bu_4N)_2[Tc_2Br_8]\cdot 4[(CH_3)_2CO]$.

to $[Tc_2Cl_8]^{2-}$ and the $[Re_2X_8]^{2-}$ ions, all of which have approximate D_{4h} symmetry. The Tc–Tc and Tc–Br distances found here are in excellent agreement with those previously determined by EXAFS spectroscopy (Table 2 and Table 3). The metal–metal separation is ~0.02 Å longer in $[Tc_2Br_8]^{2-}$ than in $[Tc_2Cl_8]^{2-}$, while the Re–Re distances are nearly identical in $[Re_2Cl_8]^{2-}$ and $[Re_2Br_8]^{2-}$. Also, the Tc–Tc distance in the quadruply bonded Tc complexes is longer than in the triply bonded ones. This phenomenon was previously discussed and it was proposed that the change from $[Tc_2Cl_8]^{3-}$ to $[Tc_2Cl_8]^{2-}$ raises the bond order but also causes a contraction of the valence orbitals of the metal atoms.[22] The contraction weakens the σ and π overlaps, which results in a lengthening of the bond and an increase of the Tc–Tc separation. The average Tc–Tc–Br angle found by XRD (105.01(3)°) is comparable to the one found by EXAFS (105.54°); this angle is slightly more obtuse than the Tc–Tc–Cl angle (103.8(4)°) in $[Tc_2Cl_8]^{2-}$.[14] Previous calculations on quadruply bonded systems have been preformed and a relationship between the M–M–X angles and the M–M distances was obtained.[23]

Table 2 Bond distances (Å), angles (°) and torsion angles (°) in the $[Tc_2Br_8]^{2-}$ ion

Bond distances/Å			
Tc(1)–Tc(1)	2.1625(9)	Tc(1)–Br(3)	2.4754(7)
Tc(1)–Br(1)	2.4796(7)	Tc(1)–Br(4)	2.4746(7)
Tc(1)–Br(2)	2.4643(7)		
Bond angles/°			
Tc(1)–Tc(1)–Br(1)	104.41(3)	Tc(1)–Tc(1)–Br(3)	105.18(3)
Tc(1)–Tc(1)–Br(2)	105.50(3)	Tc(1)–Tc(1)–Br(4)	104.95(3)
Br(1)–Tc(1)–Br(2)	150.08(3)	Br(2)–Tc(1)–Br(3)	86.88(3)
Br(1)–Tc(1)–Br(3)	86.13(3)	Br(2)–Tc(1)–Br(4)	85.42(3)
Br (1)–Tc(1)–Br(4)	86.18(2)	Br(3)–Tc(1)–Br(4)	88.3(3)
Torsion angles/°			
Br(3)–Tc(1)–Tc(1)–Br(4)	0.290(3)	Br(1)–Tc(1)–Tc(1)–Br(2)	0.813(3)
Br(1)–Br(2)–Br(3)–Br(4)	0.186(2)		

Symmetry transformations used to generate equivalent atoms: $1-x,-y+1,-z$.

Table 3 CASPT2 typical bond distances calculated with the VTZP basis set. In parentheses DFT results from Cavigliasso and Kaltsoyannis.[24] EXAFS and XRD results are also reported. Energies corresponding to the $\delta \rightarrow \delta^*$ ($^1A_{2u} \leftarrow {}^1A_{1g}$) transitions ($\Delta E$), computed also with the VQZP basis set, at the VTZP geometries

System	M–M/Å	M–X/Å	ΔE/ eV	ΔE/ cm^{-1}	Band max./ cm^{-1} [6]
$[Re_2Cl_8]^{2-}$					
$^1A_{1g}$	2.230 (2.24)	2.315 (2.34)	—	—	—
EXAFS,[25] XRD[15]	2.24, 2.222	2.36, 2.32	—	—	—
$^1A_{2u}$	2.274	2.304 (2.33)	2.063	16640	14589
VQZP	—	—	1.938	15628	—
$[Tc_2Cl_8]^{2-}$					
$^1A_{1g}$	2.211 (2.17)	2.332 (2.33)	—	—	—
EXAFS,[6] XRD[14]	2.17, 2.147	2.34, 2.320	—	—	—
$^1A_{2u}$	2.241	2.321	2.051	16547	14713
VQZP	—	—	1.963	15836	—
$[Re_2Br_8]^{2-}$					
$^1A_{1g}$	2.210 (2.24)	2.443 (2.51)	—	—	—
XRD[16]	2.218	2.473	—	—	—
$^1A_{2u}$	2.260	2.431	1.918	15471	13957
VQZP	—	—	1.840	14841	—
$[Tc_2Br_8]^{2-}$					
$^1A_{1g}$	2.174 (2.18)	2.448 (2.51)	—	—	—
EXAFS,[6] XRD	2.16, 2.162	2.48, 2.473	—	—	—
$^1A_{2u}$	2.228	2.4338	1.882	15185	13717
VQZP	—	—	1.824	14714	—

Computational

In Table 3, the CASPT2 M–M and M–X bond distances for the $^1A_{1g}$ ground state of the four species are listed, together with experimental values and the density functional theory (DFT) values obtained by Cavigliasso and Kaltsoyannis.[24] The DFT results of Kaltsoyannis *et al.* were obtained using three generalized-gradient-approximation functionals BLYP, OLYP and PBE. The CASPT2 M–M and M–X bond distances for the $^1A_{2u}$ excited are also reported in Table 3, together with the $\delta \rightarrow \delta^*$ ($^1A_{2u} \leftarrow {}^1A_{1g}$) excitation energies. The $\delta \rightarrow \delta^*$ bands for the four dimers are shown in Fig. 5. The calculated bond distances are in reasonable agreement with experiment and previous calculations. The present work adds a piece of new information to the studies performed by

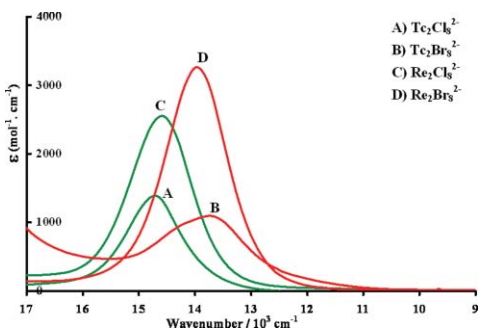

Fig. 5 The $\delta \rightarrow \delta^*$ ($^1A_{2u} \leftarrow {}^1A_{1g}$) portion of the UV-vis spectra of the $(n\text{-}Bu_4N)_2[M_2X_8]$ complexes measured in dichloromethane.

Cavigliasso and Kaltsoyannis[24] in the sense that it has allowed us to determine the properties of the $^1A_{2u}$ state with the same accuracy as the one used for the ground state. The CASPT2 excitation energies are higher than the measured values (about 2000 cm^{-1} higher with the VTZP basis set and ~1000 cm^{-1} higher with the VQZP basis set); however, the trend along the series of four compounds follows a similar pattern (Fig. 6), implying the capture of relevant systematic molecular energetic variations. The calculations nicely capture the red shift of the $\delta \rightarrow \delta^*$ transition energy going from the chlorides to the bromides, and the near degeneracy of the $\delta \rightarrow \delta^*$ energy for each pair of $[M_2Cl_8]^{2-}$ and $[M_2Br_8]^{2-}$ (M = Tc, Re) anions.

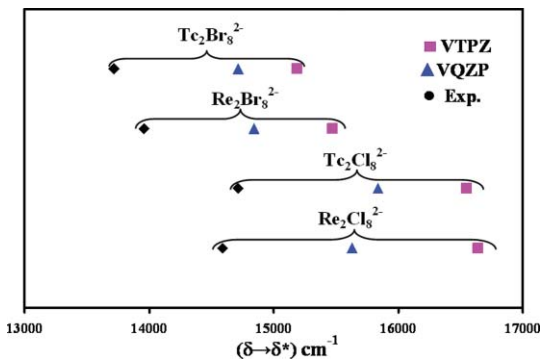

Fig. 6 Excitation energy (cm^{-1}) of the $\delta \rightarrow \delta^*$ transition for $[Re_2Cl_8]^{2-}$, $[Tc_2Cl_8]^{2-}$, $[Re_2Br_8]^{2-}$ and $[Tc_2Br_8]^{2-}$. Experimental values in black; values obtained with VTZP basis set in pink and with VQZP in blue.

In going from the VTZP to the VQZP basis set, the differences between CASPT2 and experimental excitation energies are reduced by about 500–1000 cm^{-1}. We have computed the excitation energy for $Tc_2Cl_8^{2-}$ also using a V5ZP basis set and the result differed only by 50 cm^{-1} from the result obtained with the VQZP basis set. We thus consider our results converged with respect to basis sets. The remaining difference between calculated and measured excitation energies may be due to the fact that the calculations have been performed on isolated molecules, while the optical experiments refer to salts dissolved in solution. Moreover, this energy difference is similar to what we obtained in our previous studies on the octamethyldimetalates of Cr(II), Mo(II), W(II), and Re(III).[17] We thus think that our results are as good as one can expect with this approach.

We inspected the molecular orbitals and the ground state wavefunctions for the four complexes. In Fig. 1 we present the MOs of $[Tc_2Br_8]^{2-}$ as an illustrative example. We shall start the discussion with $[Re_2Cl_8]^{2-}$. The dominant electronic configuration in the $^1A_{1g}$ ground state has a weight of 0.67, and the twelve molecular orbitals used in the calculations are nicely paired such that the sum of the occupation numbers for the bonding and antibonding orbitals of a given type is almost exactly two. We note that the two bonding Re–Cl orbitals are mainly located on Cl as expected, while the antibonding orbitals have large contributions from the Re $5d_{x^2-y^2}$ orbital. The occupation is low and these orbitals are thus almost empty and may be used as acceptor orbitals for electronic transitions. The strongest bond between the two Re atoms is the σ bond, with an occupation numbers $\eta_b = 1.92$ for the bonding natural orbital and $\eta_a = 0.08$ for the antibonding natural orbital. We can estimate the effective bond order, that can be a non integer number, as $(\eta_b - \eta_a)/(\eta_b + \eta_a)$. Thus, for the σ bond we obtain the value 0.92. The corresponding value for the π bond is 1.76. The δ/δ^* pair gives an effective bond order of only 0.57. Adding up, these numbers result in a total effective bond order of 3.25. Similar results were obtained on our previous studies of Re–Re compounds.[17] The reduction of the bond order from 4.0 to 3.25 was explained principally in terms of the weakness of the δ bond, and the concomitant correlation of the δ and δ^* orbitals. In addition, the weakly π-donating Cl^- ligands can donate into the vacant δ^* orbital, increasing its occupancy. The values of the effective bond orders (Table 4) suggest that the metal–metal bond is slightly stronger in the Re–Re case than in the Tc–Tc case.

Table 4 Effective bond order, total bond order and weight of the dominant electronic configuration in the $^1A_{1g}$ ground state for $[M_2X_8]^{2-}$ (M = Tc, Re; X = Cl, Br)

		$[Re_2Cl_8]^{2-}$	$[Tc_2Cl_8]^{2-}$	$[Re_2Br_8]^{2-}$	$[Tc_2Br_8]^{2-}$
Effective bond order	σ	0.92	0.87	0.92	0.96
	π	1.76	1.64	1.78	1.69
	δ	0.57	0.42	0.62	0.50
Total bond order		3.25	2.93	3.32	3.15
Weight of the electronic configuration in $^1A_{1g}$		0.67	0.55	0.69	0.59

Conclusions

The single-crystal X-ray structure of carmine-red $[Tc_2Br_8]^{2-}$ has been determined almost three decades after the original report of its synthesis.[26] The compound $(n\text{-}Bu_4N)_2[Tc_2Br_8]$ was prepared by dissolving $(n\text{-}Bu_4N)_2[Tc_2Cl_8]$ in aqueous acetone–HBr. The crystals that initially precipitate from solution contain acetone, which is quickly lost upon drying in air. Rapid mounting and cooling of the transparent red crystals obtained from the mother liquor enabled a successful data collection and structure determination on the crystalline solvate, $(n\text{-}Bu_4N)_2[Tc_2Br_8]\cdot 4[(CH_3)_2CO]$. The structure of $[Tc_2Br_8]^{2-}$ was previously determined *via* EXAFS methods on an acetone free sample of $(n\text{-}Bu_4N)_2[Tc_2Br_8]$ and it is gratifying that the two methods give essentially identical results for the quadruply bonded anion.[6] Other multiply bonded technetium complexes, including the two remaining members of the $[Tc_2X_8]^{2-}$ series (X = F, I), are under investigation by the collaborative team and will be reported in due course.

The molecular and electronic structures of four group 7 dinuclear $[M_2X_8]^{2-}$ (M = Re, Tc; X = Cl, Br) complexes have been investigated by multi-configurational quantum chemical methods. The calculated ground state geometries are in very good agreement with the experimentally determined values. The calculated transition energies of the $\delta \rightarrow \delta^*$ ($^1A_{2u} \leftarrow {}^1A_{1g}$) excitations are all higher than the measured values by ~1000 cm^{-1} (VQZP basis set), but the trend in the experimental values is mimicked by the calculations. The interplay between experiment and theory will be exploited in future papers in this series.

Acknowledgements

The authors thank Mr Tom O'Dou for outstanding health physics support. We also acknowledge Dr Carol J. Burns (Los Alamos National Laboratory) for a generous loan of ammonium pertechnetate. Funding for this research at UNLV was provided

by the US Department of Energy, agreement no. DE-FG52-06NA26399, and the Swiss National Science Foundation, grant no. 200020-120007.

Notes and references

1 F. A. Cotton and R. A. Walton, *Multiple Bonds between Metal Atoms, 2nd edn*, Oxford University Press, Oxford, 1993.
2 F. A. Cotton, N. F. Curtis, C. B. Harris, B. F. G. Johnson, S. J. Lippard, J. T. Mague, W. R. Robinson and J. S. Wood, *Science*, 1964, **145**, 1305.
3 A. P. Sattelberger, in *Multiple Bonds between Metal Atoms, 3rd edn*, ed. F. A. Cotton, C. A. Murillo and R. A. Walton, Springer, NY, 2005.
4 K. Schwochau, *Technetium: Chemistry and Radiopharmaceutical Applications*, Wiley-VCH, Weinheim, Germany, 2000.
5 N. A. Baturin, K. E. German, M. S. Grigor'ev and S. V. Kryuchkov, *Koordinats. Khim.*, 1991, **17**, 1375.
6 F. Poineau, A. P. Sattelberger, S. D. Conradson and K. R. Czerwinski, *Inorg. Chem.*, 2008, **47**, 1991.
7 W. Preetz, G. Peters and D. Bublitz, *J. Cluster Sci.*, 1994, **5**, 83.
8 G. M. Sheldrick, *Acta Crystallogr., Sect. A: Found. Crystallogr.*, 2008, **64**, 112.
9 G. Karlström, R. Lindh, P. A. Malmqvist, B. O. Roos, U. Ryde, V. Veryazov, P. O. Widmark, M. Cossi, B. Schimmelpfennig, P. Neograd y and L. Seijo, *Comput. Mater. Sci.*, 2003, **287**, 222.
10 B. O. Roos, R. Lindh, P. A. Malmqvist, V. Veryazov and P. O. Widmark, *J. Phys. Chem. A*, 2005, **109**, 6575.
11 B. O. Roos, P. R. Taylor and P. E. M. Siegbahn, *Chem. Phys.*, 1980, **48**, 157.
12 K. Andersson, P. A. Malmqvist and B. O. Roos, *J. Chem. Phys.*, 1992, **96**, 1218.
13 B. A. Hess, *Phys. Rev. A*, 1986, **33**, 3742.
14 F. A. Cotton;, L. Daniels, A. Davison and C. Orvig, *Inorg. Chem.*, 1981, **20**, 3051.
15 F. A. Cotton, B. A. Frenz, B. R. Stults and T. R. Webb, *J. Am. Chem. Soc.*, 1976, **98**, 2768.
16 H. W. Huang and D. S. Martin, *Inorg. Chem.*, 1985, **24**, 96.
17 L. Gagliardi and B. O. Roos, *Inorg. Chem.*, 2003, **42**, 1599.
18 F. Ferrante, L. Gagliardi, B. E. Bursten and A. P. Sattelberger, *Inorg. Chem.*, 2005, **44**, 8476.
19 B. O. Roos and L. Gagliardi, *Inorg. Chem.*, 2006, **45**, 803.
20 L. Gagliardi, *Theor. Chem. Acc.*, 2006, **116**, 307.
21 L. Gagliardi and B. O. Roos, *Chem. Soc. Rev.*, 2007, **36**, 893.
22 F. A. Cotton, K. R. Dunbar, L. R. Falvello, M. Tomas and R. A. Walton, *J. Am. Chem. Soc.*, 1983, **105**, 4950.
23 F. Mota, J. J. Novoa, J. Losada, S. Alvarez, R. Hoffmann and J. Silvestre, *J. Am. Chem. Soc.*, 1993, **115**, 6216.
24 G. Cavigliasso and N. Kaltsoyannis, *Dalton Trans.*, 2006, 5476.
25 S. D. Conradson, A. P. Sattelberger and W. H. Woodruff, *J. Am. Chem. Soc.*, 1988, **110**, 1309.
26 W. Preetz and G. Peters, *Z. Naturforsch., B*, 1980, **35**, 797.